

Electronic Supplementary Information

Cancer-targeting Gold-decorated Melanin Nanoparticles for *In vivo* Near-infrared Photothermal Therapy

Ghasidit Pornnoppadol^{1,†}, Soojeong Cho^{2,†}, Jeong Heon Yu^{1,†}, Shin-Hyun Kim^{2,*}, and Yoon Sung Nam^{1,3,*}

¹Department of Materials Science and Engineering, Korea Advanced Institute of Science and Technology, 291 Daehak-ro, Yuseong-gu, Daejeon 34141, Republic of Korea

²Department of Chemical and Biomolecular Engineering, Korea Advanced Institute of Science and Technology, 291 Daehak-ro, Yuseong-gu, Daejeon 34141, Republic of Korea

³Department of Biological Sciences, Korea Advanced Institute of Science and Technology, 291 Daehak-ro, Yuseong-gu, Daejeon 34141, Republic of Korea

† These authors equally contributed to this work

* To whom correspondence should be addressed. Email: yoonsung@kaist.ac.kr (Y.S.N.) and kim.sh@kaist.ac.kr (S.H.K.)

Estimation of heat transduction efficiency

The heat transduction from the NIR laser was calculated to determine photothermal conversion efficiency after the decoration of MNPs with AuNPs. A continuum energy balance was applied to explain the system, i.e., time-varied-temperature change is the consequence of heat energy input and output:

$$\sum_i m_i C_{p,i} \frac{dT}{dt} = Q_{NPs} + Q_o - Q_{loss} \quad (S1)$$

where C_p and m are heat capacity and mass of solutions respectively, and i denotes the system components: aqueous suspensions of MNPs or Au-MNPs in quartz cells. T is the solution temperature, and t is time. Q_{NPs} is the heat energy term induced by laser irradiation on the nanoparticles. Q_o indicates the heat dissipated to the pure solvent, and Q_{loss} is thermal energy lost.

To determine Q_{NPs} , we use

$$Q_{NPs} = I(1 - T_\lambda)\eta = I(1 - 10^{-A_\lambda})\eta \quad (S2)$$

where I is the incident laser power, A_λ is the absorbance of the solution at 808 nm, and η is the heat transduction efficiency from the light absorbed by the nanoparticles. Q_o equals 28 mW by measuring the temperature increase of water. To determine Q_{loss} , we use

$$Q_{loss} = hA\Delta T = hA(T - T_{surr}) \quad (S3)$$

where h is heat transfer coefficient and T_{surr} denotes the atmospheric temperature. To find h through an empirical method, the balance equation is modified with θ , a dimensionless temperature as described below:

$$\theta = \frac{\Delta T}{\Delta T_{max}} \quad (S4)$$

$$\frac{d\theta}{dt} = \frac{hA}{\sum_i m_i C_{p,i}} \left[\frac{Q_{NPs} + Q_s}{hA\Delta T_{max}} - \theta \right] \quad (S5)$$

The laser was turned off when the cooling curves of the system were traced. The absence of energy from the laser allows for the thermal energy term, $Q_{NPs} + Q_s$, to be removed (Fig. S4a). Therefore, the system can be described as the following equations:

$$dt = - \frac{\sum_i m_i C_{p,i}}{hA} \frac{d\theta}{\theta} \quad (S6)$$

and

$$t = - \frac{\sum_i m_i C_{p,i}}{hA} \ln \theta \quad (S7)$$

The plot of t as a function of $-\ln\theta$ has a slope of $\frac{\sum_i m_i C_{p,i}}{hA}$, which provides the value of hA (Fig. S4b). The photothermal conversion efficiency is estimated from steady-state maximum temperature:

$$Q_{NPs} + Q_s = Q_{loss} = hA\Delta T_{max} \quad (S8)$$

and

$$\eta = \frac{hA\Delta T_{max} - Q_s}{I(1 - 10^{-A\lambda})} \quad (S9)$$

MNPs with a concentration of 0.8 wt% had a photothermal conversion efficiency (η) of 40 %, and Au-MNPs with the same concentration had η of 47 %.

Average density of Au-MNPs

Au-free MNPs and Au-MNPs have different average densities so that the dispersions with the same weight fraction have different volume fractions (or number concentrations). The masses of single Au-free MNP and Au-MNP, m_{Mel} and m_{Au-Mel} , can be obtained by the following equations:

$$m_{Mel} = \rho_{Mel}V_{Mel} \quad \text{and} \quad m_{Au-Mel} = \rho_{Mel}V_{Mel} + N_{Au}\rho_{Au}V_{Au}$$

, where ρ_{Mel} and ρ_{Au} are the densities of MNP and AuNP and V_{mel} and V_{Au} are the volumes of single MNP and AuNP, and N_{Au} is the number of AuNPs per Au-MNP. The value of ρ_{Mel} is approximately 1.33 g cm⁻³ and that of ρ_{Au} is 19.3 g cm⁻³. The diameter of MNPs is 190 nm and that of AuNPs is 20 nm. As N_{Au} can be estimated as 315 from the average coverage of AuNPs of 33.9% on MNPs. Therefore, m_{Au-Mel} is approximately 5.94 times larger than m_{Mel} and the volume fraction of Au-MNPs dispersion is 5.94 times smaller than that of Au-free MNPs dispersion for the same weight fraction.

Synthesis of gold nanoparticles and gold nanorods

AuNPs were synthesized using the Turkevich method. A 100-mL sample of aqueous HAuCl₄ (0.25 mM) was prepared in a 250-mL flask, containing controlled amounts of HCl or NaOH at room temperature. The solution was brought to boil at 100°C while being stirred, and the corresponding amount of 5% aqueous sodium citrate with an initial molar ratio of citrate to Au³⁺

was added. The reaction was allowed to run until the solution reached a translucent red color, indicating the completion of the reaction.

AuNRs were synthesized by using the seed-mediated method. First, the seed solution was prepared by mixing 4.7 mL of CTAB solution (0.1 M) with 25 μ L of H_{AuCl}₄ (50 mM). To the stirred solution, 0.3 mL of ice-cold NaBH₄ (10 mM) was added, which resulted in the formation of a brownish-yellow solution. Additional stirring of the seed solution was continued for 2 min and was kept at 25 °C. Next, the growth solution was prepared by mixing 5.0 mL of CTAB solution (0.1 M) with 25 μ L of H_{AuCl}₄ (50 mM), 85 μ L of AgNO₃ (5 mM), 25 μ L of HCL (1 M), and 20 μ L of ascorbic acid (100 mM). To the stirred solution, 10 μ L of the seed solution was added and kept at 25 °C for 4 h.

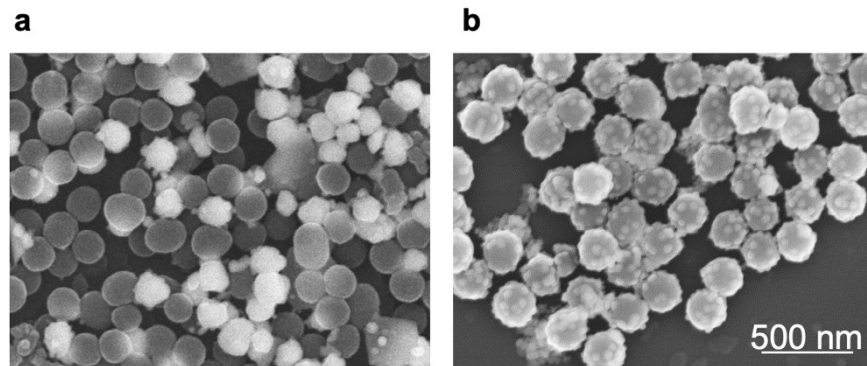


Fig. S1. Scanning electron microscopy (SEM) images of Au-MNPs, prepared with the addition of HAuCl₄ in one shot (a) and with the addition of HAuCl₄ (b).

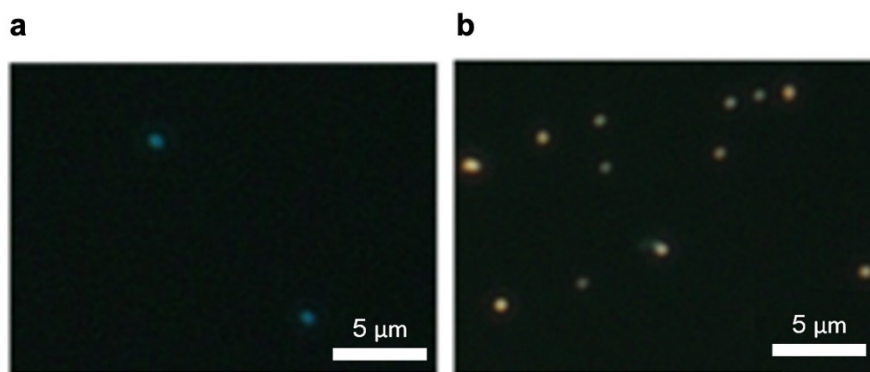


Fig. S2. Dark-field optical microscopy images of MNPs (a) and Au-MNPs (b).

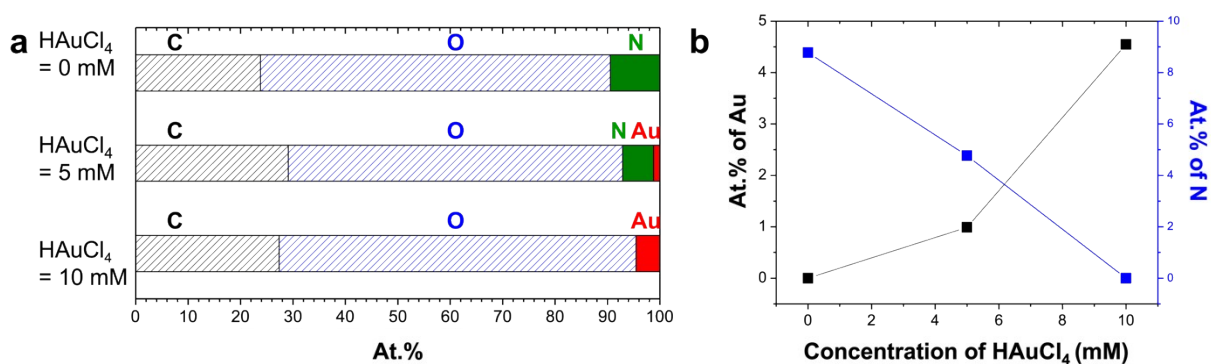


Fig. S3. Surface configuration of MNP and Au-MNP analyzed using XPS: (a) atomic composition and (b) atomic % of gold and nitrogen from three different samples prepared using the HAuCl₄ solutions with the concentrations of 0 mM (MNP), 5 mM, and 10 mM.

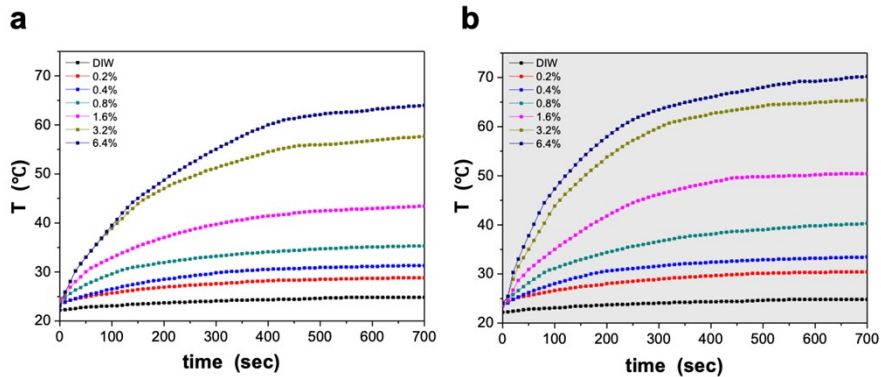


Fig. S4. The time-dependent temperature of the dispersions of MNPs (a) and Au-MNPs (b) during irradiation of an 808 nm laser with an intensity of 2.5 W cm^{-2} . Various weight fractions were used as denoted.

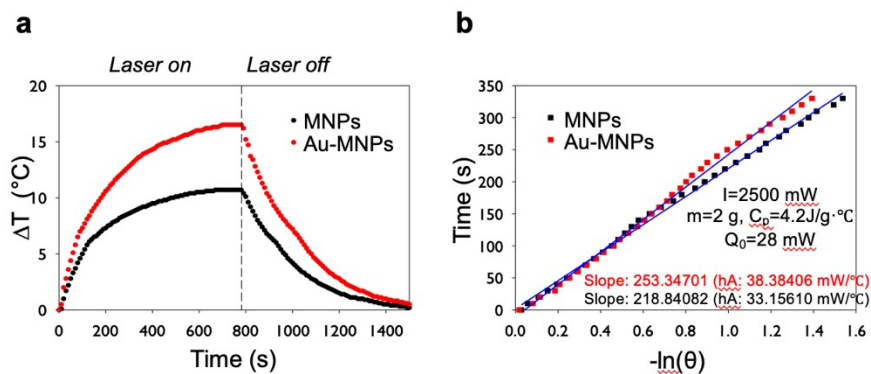


Fig. S5. (a) Time-dependent temperatures for MNPs and Au-MNPs during laser irradiation and off. (b) Plots for a time as a function of $-\ln(\theta)$, of which slope was used to estimate the values of hA .

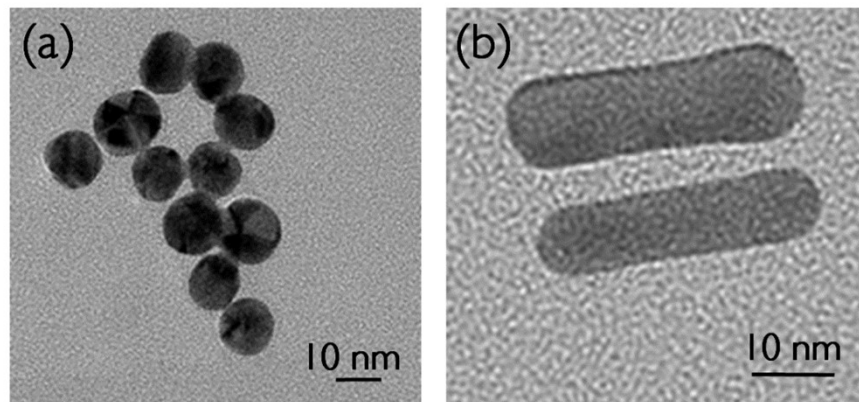


Fig. S6. TEM images of AuNPs (a) and AuNRs (b).

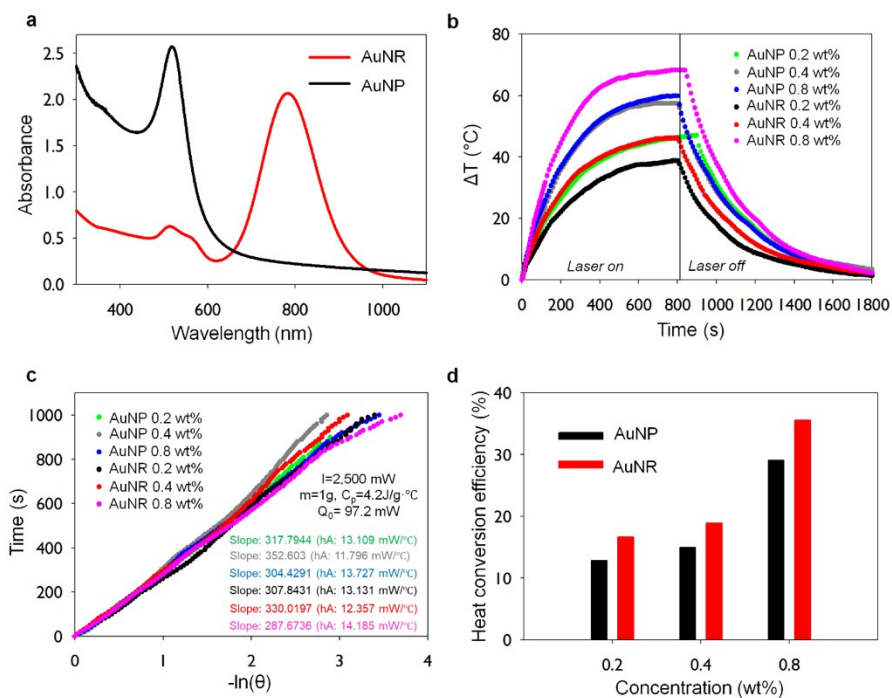


Fig. S7. Absorption spectra (a) and time-dependent temperatures (b) of AuNPs and AuNRs during laser on and off (c) Linear time data versus $-\ln(\theta)$ of AuNPs and AuNRs obtained from the cooling period. (d) Concentration-dependent heat conversion efficiencies of AuNPs and AuNRs.

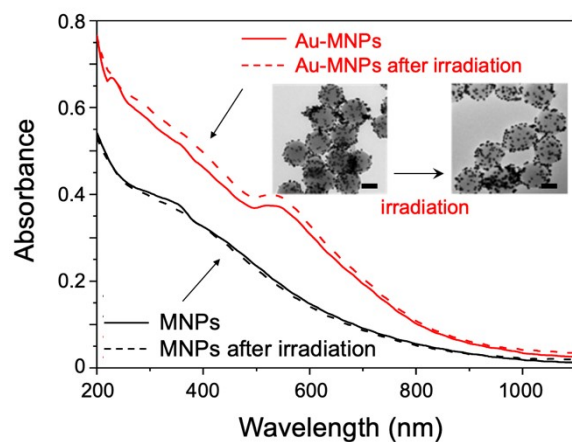


Fig. S8. Absorption spectra of MNPs and Au-MNPs before and after laser irradiation for 30 min. Insets are TEM images of MNPs and Au-MNPs before and after irradiation. Scale bars are 100 nm.

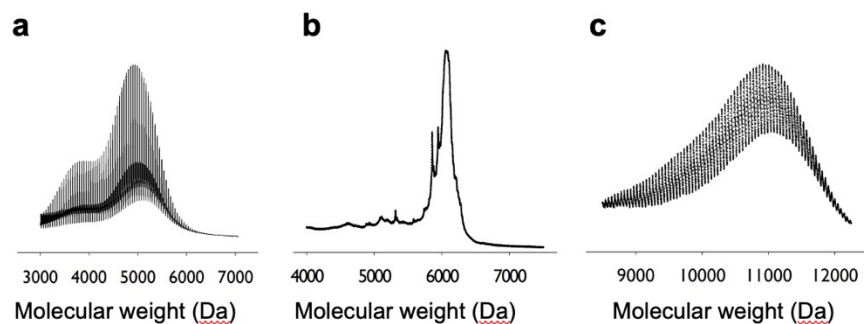


Fig. S9. Matrix-assisted laser desorption/ionization-time-of-flight (MALDI-TOF) mass spectrometry spectra of PEG (a), EGF (b), and EGF-PEG conjugate (c), respectively.

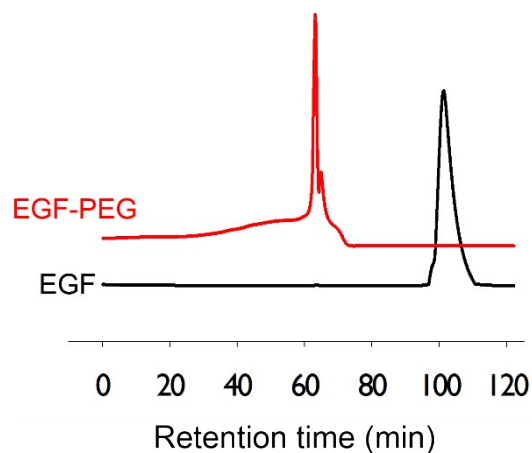


Fig. S10. RP-HPLC diagrams of EGF and EGF-PEG

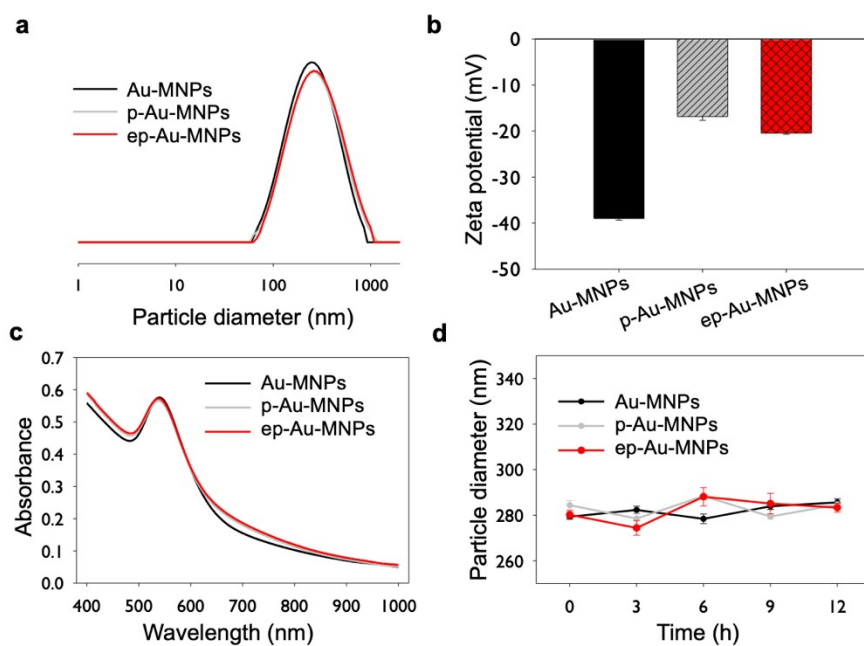


Fig. S11. Normalized size distribution (a), zeta potential (b), absorption spectra (c), and temporal size changes (d) of Au-MNPs, p-Au-MNPs, and ep-Au-MNPs dispersed in the serum.

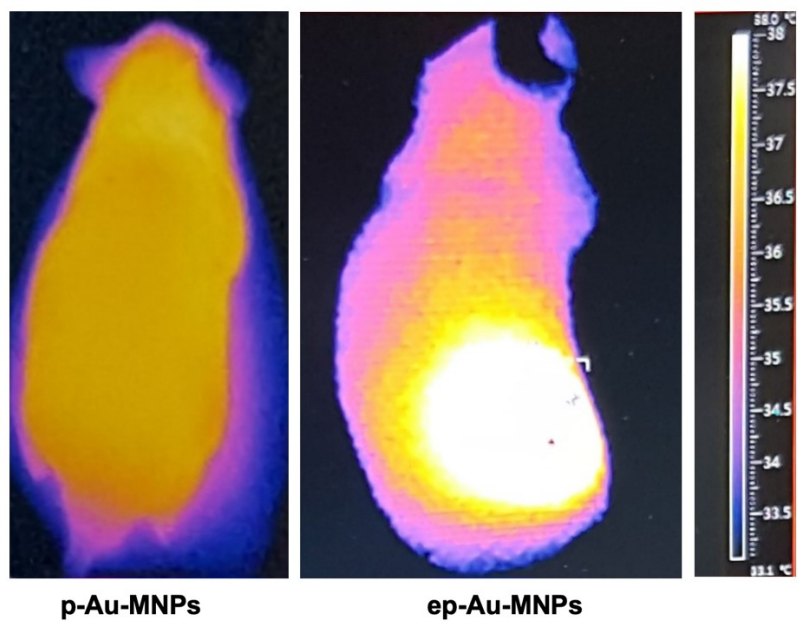


Fig. S12. Photothermal images of mice injected with p-Au-MNPs and ep-Au-MNPs captured from the FLIR camera

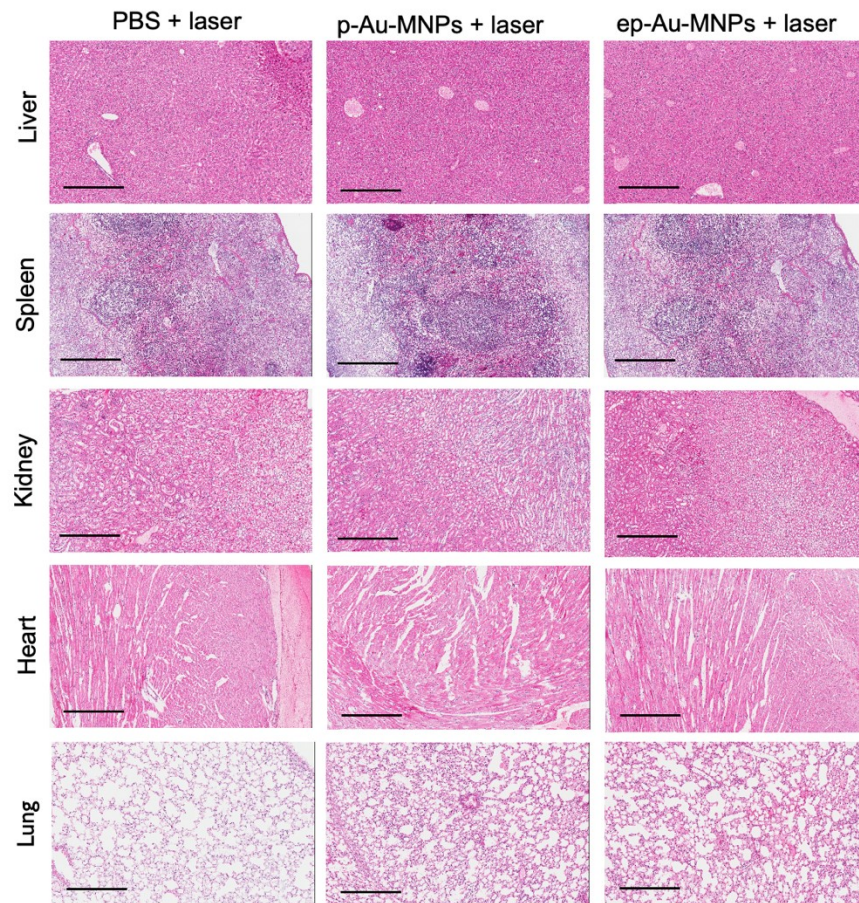


Fig. S13. Toxicity assessment of the main organs with H&E staining. After laser irradiation, no obvious tissue damage was observed (scale bar = 400 μm).